Evidence for a myotomal Hox/Myf cascade governing non-autonomous control of rib specification within global vertebral domains

Tânia Vinagre[1], Natalia Moncaut[1,$], Marta Carapuço[1,#], Ana Nóvoa[1], Joana Bom[1], Moisés Mallo[1,2]

Correspondence: Moises Mallo

mallo@igc.gulbenkian.pt

Phone: +351 214 464 624

Fax: +351 214 407 970

Running Title: Hox-mediated control of rib formation

1 Instituto Gulbenkian de Ciência. Rua da Quinta Grande 6. 2780-156 Oeiras. Portugal
2 Department of Histology and Embryology, School of Medicine, University of Lisbon
$ Current address: Section of Gene Function and Regulation, The Institute of Cancer Research, Chester Beatty Laboratories, London SW3 6JB, United Kingdom.
 # Current address: Unidade de Morfogenese e Reparação de Tecidos, Instituto de Medicina Molecular, Universidade de Lisboa, Av. Professor Egas Moniz, 1649-028 Lisbon, Portugal

Abstract

Hox genes are essential for the patterning of the axial skeleton. Hox group 10 has been shown to specify the lumbar domain by setting a rib-inhibiting program in the presomitic mesoderm (PSM). We have now produced mice with ribs in every vertebra by ectopically expressing Hox group 6 in the PSM, indicating that Hox genes are also able to specify the thoracic domain. We show that the information provided by Hox genes to specify rib-containing and rib-less areas is first interpreted in the myotome through the regional specific control of *Myf5* and *Myf6* expression. This information is then transmitted to the sclerotome by a system that includes FGF and PDGF signaling to produce vertebrae with or without ribs at different axial levels. Our findings offer a new perspective of how Hox genes produce global patterns in the axial skeleton and support a redundant non-myogenic role of *Myf5* and *Myf6* in rib formation.

Introduction

Hox genes have been classically described to be involved in the production of vertebrae with individual characteristics (Krumlauf 1994; Wellik 2007; Mallo et al. 2009). More recently, it was discovered that Hox genes also play essential roles in defining global vertebral domains (Wellik and Capecchi 2003). In particular, it was shown that Hox group 10 is responsible for the layout of the rib-less lumbar region by diverting it from a rib-containing thoracic identity (Wellik and Capecchi 2003; Carapuço et al. 2005). In addition, Hox group 11 was demonstrated to be required for the formation of the sacrum (Wellik and Capecchi 2003). However, it remains unclear whether or not Hox genes are involved in the global specification of the thoracic and cervical domains. Moreover, the mechanism by which Hox genes control these processes is completely unknown.

Wellik and Capecchi (2003) proposed that ribs are set out by default and that the rib-less cervical domain would result from the rib-blocking activity of other Hox genes acting similarly to Hox group 10 in the lumbar region. However, this hypothesis is difficult to reconcile with published expression patterns for Hox genes (Burke et al. 1995), which instead suggest an alternative hypothesis. In particular, the anterior limit of expression of members of the Hox group 6 correlates with the cervical to thoracic transition in a variety of vertebrates bearing a different number of cervical vertebrae (Burke et al. 1995), indicating that this Hox group might have a role in promoting rib formation. Here we present evidence supporting this hypothesis, showing that Hox control of rib formation is mediated by regulation of *Myf5* and *Myf6* expression in the hypaxial myotome through the interaction with a relevant enhancer. Moreover, our transgenic analyses indicate that myotomal *Myf5*/*Myf6* activation triggers a non-autonomous effect mediated by PDGF

and FGF signaling, promoting rib formation in the adjacent sclerotome. Our data supports a redundant non-myogenic role of *Myf5* and *Myf6* in the processes leading to rib formation.

Results

Over-expression of Hox group 6 induces ectopic rib formation

In order to test whether Hox group 6 activity could induce rib formation, we employed a transgenic approach to over-express *Hoxb6* either in the presomitic mesoderm (PSM) or in the somites of mouse embryos. Whilst somite-exclusive expression gave mild phenotypes (Fig. S1A, B), the extended expression of *Hoxb6* in PSM cells resulted in the formation of ectopic ribs throughout the whole length of the axial skeleton (Fig. 1A, B), without affecting the total number of vertebrae. In these transgenics, the prospective cervical area contained ribs fused laterally to form an apparent articular surface for the forelimbs, which were slightly displaced rostrally. The prospective lumbar area also displayed ectopic ribs, progressively decreasing in size in a caudal direction, presumably following the physiological decrease in size of the lower thoracic ribs. In the presumptive sacral area, the vertebrae lost their characteristic morphology and assumed rib-like features, while keeping the lateral fusions typical of the sacral region.

The normal expression of Hox group 10 genes seen in *Dll1-Hoxb6* transgenics (Fig. S1C-E) indicates that the rib phenotype of *Dll1-Hoxb6* embryos does not result from down-regulation of Hox group 10 genes, despite the similarities in the phenotypes of these transgenics compared to the global group 10 deletion mutants (Wellik and Capecchi 2003). Therefore, Hox paralog groups 6 and 10 seem to modulate the processes leading to

rib formation in antagonistic ways. Hence, the "snake-like" (*Dll1-Hoxb6*) transgenics together with our previously described rib-less (*Dll1-Hoxa10*) embryos (Carapuço et al. 2005) provide a complementary system to study how Hox genes control rib formation.

Hox groups 6 and 10 control regional hypaxial expression of genes in the *Myf5*/*Myf6* pathway

Because ribs derive from the sclerotome (Huang et al. 2000), we expected this somitic compartment to be affected in our transgenics. However, we found no significant differences in the expression patterns of sclerotomal markers such as *Pax1*, *Pax9* and *Meox2* in the Hox transgenics (Fig. S1F-N). Hence, we decided to analyze the expression of genes that have been associated with rib deficiencies in genetic studies. Several mutations of the myogenic factor *Myf5* have been produced and, whereas myogenesis remains relatively normal, some mutants displayed strong rib defects that resembled the phenotypes observed in our *Dll1-Hoxa10* transgenics (Braun et al. 1992; Tajbakhsh et al. 1996; Carapuço et al. 2005). In wild-type embryos, *Myf5* expression follows specific regional patterns. While it is expressed in the dorso-medial (epaxial) myotome of somites at all rostro-caudal levels, it is only detected in the ventrolateral (hypaxial) myotome of somites located between the limb buds, which are those producing rib-bearing vertebrae (Fig. 1C, C', E, E' and Fig. S1O, O'). In both *Dll1-Hoxa10* and *Dll1-Hoxb6* transgenic embryos the distribution of *Myf5* transcripts was clearly affected. Interestingly, the changes in *Myf5* expression were region-specific, correlating with the relative changes seen in rib development. In *Dll1-Hoxa10* transgenics *Myf5* was down-regulated specifically in the hypaxial myotome of interlimb somites (prospective thoracic region)

(Fig. 1D, D'), and in *Dll1-Hoxb6* transgenic embryos *Myf5* was ectopically activated in the ventrolateral domain of somites at limb and neck levels (prospective rib-less regions) (Fig. 1 F, F' and Fig. S1P, P'). Thus, we observe a strong positive correlation for rib development and hypaxial *Myf5* expression.

Mutations in *Myf6* have also been associated with severe rib deficiencies resembling those seen in *Dll1-Hoxa10* transgenics (Braun and Arnold 1995), indicating that this gene could also be a target of Hox gene activity. Expression analysis showed patterns similar to those observed for *Myf5*. In *Dll1-Hoxa10* transgenic embryos, *Myf6* was severely down-regulated, most prominently in the hypaxial myotome of the interlimb area (Fig. 1G, G', H, H'; see also Fig. 3A', B'). Conversely, we found ectopic *Myf6* activation in the hypaxial myotomal domain of somites at limb and neck levels in *Dll1-Hoxb6* transgenics (Fig. 1I, I', H, H' and Fig. S1Q, Q', R, R'). Interestingly, hypaxial expression at the hindlimb level of *Dll1-Hoxb6* transgenics preceded that of the epaxial domain (Fig. S1R, R'), thus mimicking the temporal pattern that has been described for the interlimb region in wild-type embryos (Summerbell et al. 2002). Together, these results indicate that Hox groups 6 and 10 are able to control *Myf5* and *Myf6* regional specific expression in the hypaxial myotome in a pattern that closely correlates with rib development. Interestingly, in situ analysis of *Myf5* mutants with normal ribcages (Kaul et al. 2000; we will refer to these mutants as $Myf5^{\Delta loxp/\Delta loxp}$) revealed that while *Myf6* expression was down-regulated in the epaxial myotome, expression of *Myf6* in the hypaxial myotome of interlimb somites was clearly conserved (Fig. 2A, A', B, B'), displaying a pattern complementary to that found in *Dlll1-Hoxa10* transgenics. Altogether, these results indicate that Hox genes are able to control the expression of *Myf5* and *Myf6* in the

domain that is relevant for rib formation and are consistent with a redundant role for these genes in rib induction.

To further evaluate *Myf5*/*Myf6* activity in the Hox transgenics, we tested the expression of suggested downstream effectors. We first assayed *Pdgfa* and *Fgf4*, which were shown to be down-regulated in *Myf5* mutant embryos (Grass et al. 1996; Tallquist et al. 2000). Expression of these genes followed patterns similar to those described for *Myf5* and *Myf6*. In *Dll1-Hoxa10* embryos these growth factors failed to be activated in the hypaxial domain of interlimb somites, while the remaining expression domains appeared largely unaffected (Fig. 2G-J). Conversely, *Dll1-Hoxb6* embryos presented ectopic *Pdgfa* and *Fgf4* expression in the hypaxial domain of limb and neck somites (Fig. 2K-N; FigS2A-B'). We also observed that *Pdfga* and *Fgf4* expression was conserved almost exclusively on the hypaxial myotome of interlimb somites of $Myf5^{\Delta loxp/\Delta loxp}$ embryos, although the levels were lower than in control specimens (Fig. 2C-F).

Interestingly, not all *Myf5* targets were similarly affected in the Hox transgenic embryos. Myogenin (*Mgn*), a *Myf5* target gene in the myogenic cascade (Pownall et al. 2002), was up-regulated in the ventrolateral myotome of limb and neck somites of *Dll1-Hoxb6* transgenics but its expression was not affected in *Dll1-Hoxa10* embryos (Fig. S2C-F). While the *Mgn* pattern observed in *Dll1-Hoxb6* embryos could result from activation by *Myf5*/*Myf6*, the fact that *Mgn* is not down-regulated in *Dll1-Hoxa10* interlimb hypaxial somites can be attributed to normal *MyoD* expression (Fig. S2G, H), which is also upstream of *Mgn* (Pownall et al. 2002). The persistent hypaxial expression of myogenic genes like *MyoD* and *Mgn* in *Dll1-Hoxa10* transgenics is consistent with the presence of muscles in the whole circumference of the prospective thoracic area of these transgenics

(Fig. S2M). In addition, induction of an interlimb-like *Mgn* expression pattern in the hypaxial myotome at forelimb and neck levels of *Dll1-Hoxb6* transgenics is in agreement with the presence of intercostal muscles associated with the ribs in the neck of these transgenics (Fig. S2N, O). Further analysis of the *Dll1-Hoxa10* embryos with additional myotomal markers, such as *Six1* or *Pax3*, also revealed no significant differences when compared to wild-type littermates (Fig. S2I-L).

These results suggest that the effect of Hox groups 6 and 10 is quite specific for *Myf5*/*Myf6* and not a result of a general effect on the myotome. Furthermore, the expression of *Fgf4* and *Pdgfa* in *Dll1-Hoxa10* and $Myf5^{\Delta loxp/\Delta loxp}$ embryos suggests their involvement in a *Myf5*/*Myf6*-specific pathway associated with rib development.

Hypaxial *Myf6* expression rescues the rib-less *Dll1-Hoxa10* phenotype

To determine if the Hox-modulated expression of *Myf5*/*Myf6* is key to rib development, we tested whether *Myf6* could rescue the rib-less *Dll1-Hoxa10* phenotype when expressed in the hypaxial somite. As *Pax3* expression seems to be unaffected by *Hoxa10* (Fig. S2K, L), we used an enhancer of this gene that promotes expression in the hypaxial somite (Brown et al. 2005). *Pax3Pr-Myf6* transgenic embryos showed no apparent skeletal phenotype, which was expected since the hypaxial *Pax3* enhancer reproduces the normal expression of this gene in the hypaxial somite at the different axial levels (Brown et al. 2005) (Fig. 3A'-C'). For the rescue experiment we produced *Pax3Pr-Myf6*::*Dll1-Hoxa10* double transgenics. Three of the seven double transgenics generated had recognizable rib phenotypes, which were much less severe than those observed in *Dll1-Hoxa10* transgenics. In particular, while *Dll1-Hoxa10* transgenics showed strong rib

phenotypes, typically a complete absence of ribs in 65% of the cases (Fig. 3B; Table 1; Carapuço et al. 2005), *Pax3Pr-Myf6*::*Dll1-Hoxa10* double transgenics showed a mild alteration in the total number of ribs combined with the presence of variable abnormal patterns such as rib fusions, proximal gaps and distorted rib insertions in the sternum (Fig. 3C, Tables 1 and S1). This result indicates that *Myf6* expression in the hypaxial somite is sufficient to rescue the *Hoxa10*-induced rib phenotype, thus, providing further evidence of a direct contribution of this myogenic factor to the rib phenotypes obtained in the Hox transgenics and its involvement in rib development.

Binding of Hox groups 6 and 10 proteins to an enhancer that drives hypaxial expression of *Myf5*.

Among the different control regions that have been described for *Myf5*, an enhancer was identified that drives expression in the somitic domain affected in our Hox transgenics (Bajard et al. 2006; Buchberger et al. 2007; Giordani et al. 2007). The homology element 1 (H1) of this enhancer (Buchberger et al. 2007), also known as 147 bp enhancer (Bajard et al 2006), contains the sequence CTAATTG, which fits with predicted target sequences for Hoxb6 and Hoxa10 (Noyes et al. 2008). This potential Hox-binding site seems to be required for enhancer activity according to transgenic reporter assays (Buchberger et al. 2007). To test if our candidate Hox proteins bind this enhancer in vivo, we performed chromatin immunoprecipitation experiments on PSM isolated from mouse embryos. We could consistently immunoprecipitate the H1 enhancer element but not other genomic areas using specific antibodies for both Hox group 6 and 10 proteins (Fig. 3D). This result suggests a physiological positioning of these Hox proteins at a genomic region that

drives *Myf5* expression in the hypaxial myotomal domain and is consistent with a Hox-mediated regulation of *Myf5* in this embryonic region.

When tested using a luciferase reporter assay in cultured cells, both Hoxa10 and Hoxb6 fused to VP16 activated transcription from the wild type H1 enhancer, but not from a mutant version of this element lacking the Hox-binding site (Fig 3E), further validating the capability of Hox proteins to bind to the CTAATTG sequence of the H1 enhancer. The mutant version of H1 used in these experiments still contained intact the Pax3 and Six1-binding sites also present in this enhancer, indicating that the CTAATTG site is the main target sequence for Hox proteins in this regulatory element.

Discussion

In this study we show that specification of global vertebral domains in the vertebrate axial skeleton is controlled by the balanced activity of different Hox genes. It had been previously shown that Hox groups 10 and 11 play essential roles in the patterning of the lumbar and sacral regions, respectively (Wellik and Capecchi, 2003; Carapuço et al. 2005). Our results now indicate that Hox genes of the paralog group 6 are able to provide the instructions to generate the thoracic area. According to our data, the presence of ribs is not a default state (Wellik and Capecchi, 2003) but rather the result of a positive activity of Hox genes that triggers processes leading to rib induction. In caudal areas Hox group 10 proteins override this activity to generate the rib-less areas of the skeleton. In our model, the cervical domain is passively determined as the region anterior to the start of the rib-determining Hox activity (Fig. S3).

Surprisingly, we found that the primary target of the rib-forming/rib-blocking activities of Hox genes does not seem to be the sclerotome, but rather specific genes expressed in the myotomal compartment. In particular, we show that the primary targets of Hox genes are *Myf5* and *Myf6* specifically in the hypaxial myotome. This implies a non-myogenic function of *Myf5*/*Myf6* that controls rib development. The role of *Myf5* in rib formation has been a matter of controversy. Initial studies pointed to *Myf5* as a central player in the processes leading to rib development (Braun et al. 1992). However, when other *Myf5* mutants were produced that exhibited no rib defects (Kaul et al. 2000), it was suggested that the rib determining factor was not *Myf5* itself but another gene somehow linked to it. A decade later, such a gene has not been identified and recent new data once more associated *Myf5* with rib development (Gensch et al. 2008; Haldar et al. 2008). Among the genes located close to *Myf5* in the genome only *Myf6* stands out as a candidate to be involved in rib development since rib phenotypes have been described in some mutants for this gene (Braun and Arnold 1995; Patapoutian et al. 1995; Zang et al. 1995). Interestingly, rib deficiencies have been observed only when inactivation of either *Myf5* or *Myf6* also affected expression of the other gene (Braun et al. 1992; Braun and Arnold 1995; Patapoutian et al. 1995; Tajbakhsh et al. 1996; Zang et al. 1995; Yoon et al. 1997; Kassar-Duchossoy et al. 2004; and this manuscript). This suggests that *Myf5* and *Myf6* have redundant functions in rib formation and that it is the double inactivation of both genes that causes the rib phenotypes in particular *Myf5* and *Myf6* mutants, rather than the effects on an additional rib-determining gene in the *Myf* genomic area. Our results with both *Dll1-Hoxa10* transgenics and $Myf5^{\Delta loxp/\Delta loxp}$ mutants are fully consistent with this hypothesis. In addition, the involvement of the Myf factors in rib development is also

supported by the ability of *Myf6* to rescue the rib-less *Dll1-Hoxa10* phenotype, when expressed in the hypaxial somite.

Our observations that Hox-driven information seems to be first interpreted by a specific population of myotomal *Myf5*/*Myf6*-expressing cells could indicate that these cells can directly contribute to the ribs. However, while cell tracing experiments have shown contribution of *Myf5*-expressing cells to the ribs (Gensch et al. 2008; Haldar et al. 2008), they seem to represent a rather small fraction of the rib chondrocytes to fully explain *Myf5* contribution to rib development. In addtion, *Myf6*-expressing cells were not found in the sclerotomal compartment using a similar cell tracing strategy (Haldar et al 2008). Therefore, it seems more likely that the *Myf5*/*Myf6*-expressing cells convey their rib-forming information to the sclerotome through a cell non-autonomous mechanism. Our results suggest that members of the FGF and PDGF signaling pathways are involved in this mechanism, an idea that is also supported by genetic studies consistent with the participation of FGFs and PDGFs in rib formation. In particular, inactivation of *Pdgf-alpha* receptor resulted in severe rib anomalies (Soriano 1997) and insertion of a *Pdgfa* cDNA in the *Myf5* locus significantly rescued the *Myf5* rib phenotype (Tallquist et al. 2000). The involvement of *Fgf4* in rib formation has not been genetically addressed but a variety of experiments performed in chicken embryos suggest that FGF signaling is important for rib formation (Huang et al. 2003). Altogether, these results strongly suggest that FGF and PDGF signaling are important components of the mechanism that transmits patterning information from *Myf5*/*Myf6* to the sclerotome.

Regulation of *Myf5*/*Myf*6 by Hox genes may be a complex process. While the activity of *Hoxa10* and *Hoxb6* seems to be required before somites are formed, their effect is only

detected at a later developmental stage in a specific somitic domain. This observation seems to be at odds with a simple transcriptional activation (Hoxb6) or repression (Hoxa10) mechanism, as it is the normal expression of *Myf5* and *Myf6* in the tail tip of *Dll1-Hoxb6* transgenics (Fig. S1E). Therefore, Hox proteins must functionally interact with other factors to modulate spatial and temporally specific activity of the *Myf5*/*Myf6* regulatory region. Pax3 and Six1/4 are likely candidates to be involved in this process, as they also interact functionally with the H1 enhancer through binding sites located at both sides of the Hox site (Bajard et al. 2006; Giordani et al. 2007). Interestingly, expression of a dominant negative version of Pax3 from the *Pax3* locus down-regulated *Myf5* and *Myf6* expression in the hypaxial myotome of interlimb somites without affecting other myogenic factors like *MyoD* or *Mgn* (Bajard et al. 2006), which resembles our observations in *Dll1-Hoxa10* transgenics. This suggests that *Hoxa10* activity could involve functional inactivation of *Pax3*. If this is the case, it cannot occur at the transcriptional level, as *Pax3* expression seemed normal in *Dll1-Hoxa10* transgenics. Direct competition for binding to the enhancer is also unlikely because *Hoxa10* activity is observed when this gene is expressed in the PSM and not in the somites (Carapuço et al., 2005), and *Pax3* is only expressed in the somites. A similar spatial-temporal gap is observed between *Pax3* expression and *Hoxb6* activity in the transgenics. This suggests a sequential activity of Hox proteins and Pax3 (and probably Six1/4) to activate *Myf5*/*Myf6* expression in the hypaxial myotome. A possible scenario is that Hox proteins provide a label to the *Myf5*/*6* hypaxial enhancer, which would promote (Hoxb6) or block (Hoxa10) binding and/or activation by Pax3 later in the differentiating somite, eventually regulating *Myf5*/*Myf6* expression. Interestingly, a "label based" mechanism to modulate of cell type-

specific recruitment of transcription factors to distal enhancers has been recently reported (Lupien et al. 2008). Experiments are currently in progress to test if Hox/Pax3 interactions are also mediated through an equivalent mechanism. Of note, interactions between Hox and Pax proteins with differential functional outcomes have also been described for other members of the Hox and Pax families (Yallowitz et al. 2009). Therefore, Hox-Pax functional interactions could be a general theme in vertebrate development.

It has been suggested that regulation of hypaxial *Myf5* expression by *Pax3* might require, in addition to the H1 enhancer, other still not identified earlier acting elements (Bajard et al. 2006). Similarly, it is possible that Hox-mediated modulation of *Myf5*/*Myf6* expression in the hypaxial myotome could involve additional components, which is consistent with the complex regulation of the *Myf5*/*Myf6* locus (Carvajal et al. 2008). A probable location for such elements is the genomic region between 88 and 140 kb upstream of the *Myf5* gene, which has been reported to contain early hypaxial enhancers (Carvajal et al. 2001).

The Hox-mediated patterning process we describe in this manuscript serves as a mechanism for the establishment of global vertebral domains (i.e., cervical, thoracic, lumbar) through the specification of rib-containing and rib-less areas of the skeleton. Whether Hox genes use a similar mechanism to specify the individual features that characterize the different vertebrae, or this is elicited by direct control of sclerotomal development, remains to be determined. However, the primary involvement of myotomal components in the specification of global vertebral domains provides an evolutionarily efficient mechanism that ensures the concomitant evolution of the ribs and their

associated muscles, to produce animals with properly organized axial musculoskeletal systems. Curiously, rib development in turtles follows a plan that differs from that typically observed in other amniotes, resulting in the formation of the carapace. This specific rib development is associated with turtle-specific *Myf5* hypaxial expression in the trunk (Ohya et al. 2006) and development of specific muscle attachments (Nagashima et al. 2009), further suggesting the importance of the *Myf5*-rib connection in the evolution of the body plan.

Experimental Procedures

The *Dll1-Hoxa10* construct was previously described (Carapuço et al. 2005). The *Sm-Hoxb6* and *Dll1-Hoxb6* constructs were generated by insertion of the human *Hoxb6* cDNA (IMAGE: 4548382) downstream of the *Sm* (Carapuço et al. 2005) and *Dll1* (Beckers et al. 2000) enhancers, respectively, and upstream of the SV40 polyadenylation signal. The *Pax3Pr-Myf6* construct was generated by cloning the *Myf6* cDNA (IMAGE: 8733960) downstream of the hypaxial enhancer of the *Pax3* gene (Brown et al. 2005) and upstream of the SV40 polyadenylation signal. Transgenic embryos were produced by pronuclear injection according to standard methods. All transgenic mice used in this work have a FVB/N genetic background. Of note, normal fetuses derived from our FVB/N colony present a slight deviation from the typical axial formula, as they contain a small rib in L1 with a penetrance of about 60%, which is also observed in non-affected transgenics with this genetic background. The $Myf5^{\Delta loxp/\Delta loxp}$ mutants have been previously described (Kaul et al. 2000). Fetuses were dissected at E18.5 and skeletal preparations made using the alcian blue/alizarin red staining method (Mallo and Brändlin 1997).

Whole mount in situ hybridization (ISH) was performed as described elsewhere (Kanzler et al. 1998). ISH-stained embryos were embedded in gelatin/albumin and sectioned with a vibratome.

Chromatin immunoprecipitation assays were performed using PSM from E9.5 mouse embryos. Briefly, PSM were dissected in PBS and fixed in 1% formaldehyde. After tissue homogenization, samples were sonicated and immunoprecipitated using Hoxc6 antibody (Abcam ab41587), Hoxa10 antibody (kindly provided by J. Dasen) or control rabbit IgG (Abcam ab27478), pre-bound to Dynabeads Protein A (Invitrogen). The immunoprecipitated DNA was PCR-amplified using primers for the H1 enhancer: GCCATCTACTCTCACACACCATAC and CCACGCTAAAATACAGACATGCAG; and for a negative control region: CTGGCGTGTCTCCCTCTCTGCTGAA and GCTCCGAAGGCTGCTACTCTTGGCT.

For the luciferase assays, reporter plasmids were made by cloning the wild type or a mutant version of the H1 enhancer in which the CAATTA was replaced for CGCGCTG upstream of the minimal promoter of the pGL3-Promoter Vector plasmid. Transfections were performed on 293T cells using reporter plasmids together with plasmids expressing either VP16:Hoxa10, VP16:Hoxb6 or, as a control, the tetracycline transactivator (tTA) (Gossen and Bujard, 1992) using Lipofectamine 2000. The pCMV-β plasmid was included in all electroporations for normalization. Luciferase activity was measured on cell extracts 24h after transfection and normalized to β-galactosidase activity. Significance was evaluated using Student's t-test.

To quantify transcript levels, total RNA was extracted with Trizol (Sigma) according to the manufacturer's protocol. cDNAs were synthesized by random priming using

Superscript II reverse transcriptase (Invitrogen) and the mRNA levels were determined by qPCR using QuantifastTM FYBR® Green PCR Kit (Qiagen). The primers used were *Hoxa10*F: AGCGAGTCCTAGACTCC and *Hoxa10*R: GTCCGTGAGGTGGACGCTACG; *Hoxa11*F: AACTTCAAGTTCGGACAGCGG and *Hoxa11*R: TCAGTGAGGTTGAGCATGCGG; *Myf5*F: TCCTCAGGAATGCCATCCGC and *Myf5*R: GACAGTAGATGCTGTCAAAG; and *Myf6*F: AGACTGCCCAAGGTGGAGAT and *Myf6*R: AATGTTCCAAATGCTGGCTG.

Acknowledgments

We would like to thank J. Carvajal for the *Myf5* probe and for the *Myf5*$^{\Delta loxp/\Delta loxp}$ embryos, P. Gruss for the *Pax3* probe, N. Bobola for the *Six1* probe, A. Kispert for the *Mgn* probe, G. Martin for the *Fgf4* probe, A. Gossler for the *Dlll* promoter, J. Dasen and T. Jessell for the Hoxa10 antibody, and J. Rowland and R. Cassada for reading the manuscript. This work was supported by grants PTDC/BIA-BCM/71619/2006 to MM and by Centro de Biologia do Desenvolvimento POCTI-ISFL-4-664. TV was supported by SFRH/BD/27306/2006 and NM by SFRH/BPD/26668/2006.

References

Bajard, L., Relaix, F., Lagha, M., Rocancourt, D., Daubas, P. and Buckingham, M. E. (2006). A novel genetic hierarchy functions during hypaxial myogenesis: Pax3 directly activates Myf5 in muscle progenitor cells in the limb. Genes Dev. 20, 2450-2464.

Beckers, J., Caron, A., Hrabé de Angelis M., Hans S., Campos-Ortega J.A., and Gossler A. (2000). Distinct regulatory elements direct delta1 expression in the nervous system and paraxial mesoderm of transgenic mice. Mech. Dev. 95, 23-34.

Braun, T. and Arnold, H. H. (1995). Inactivation of Myf-6 and Myf-5 genes in mice leads to alterations in skeletal muscle development. EMBO J. 14, 1176-1186.

Braun, T., Rudnicki, M. A., Arnold, H. H. and Jaenisch, R. (1992). Targeted inactivation of the muscle regulatory gene Myf-5 results in abnormal rib development and perinatal death. Cell 71, 369-382.

Brown, C. B., Engleka, K. A., Wenning, J., Min Lu, M. and Epstein, J. A. (2005). Identification of a hypaxial somite enhancer element regulating Pax3 expression in migrating myoblasts and characterization of hypaxial muscle Cre transgenic mice. Genesis 41, 202-209.

Buchberger, A., Freitag, D. and Arnold, H. H. (2007). A homeo-paired domain-binding motif directs Myf5 expression in progenitor cells of limb muscle. Development 134, 1171-1180.

Burke, A. C., Nelson, C. E., Morgan, B. A. and Tabin, C. (1995). Hox genes and the evolution of vertebrate axial morphology. Development 121, 333-346.

Carapuço, M., Nóvoa, A., Bobola, N. and Mallo M. (2005). Hox genes specify vertebral types in the presomitic mesoderm. Genes Dev. 19, 2116-2121.

Carvajal, J. J., Cox, D, Summerbell, D. and Rigby, P. W. J. (2001). A BAC transgenic analysis of the Mrf4/Myf5locus reveals interdigitated elements that control activation and maintenance of gene expression during muscle development. Development 128, 1857-1868.

Carvajal, J. J., Keith, A. and Rigby, P. W. (2008). Global transcriptional regulation of the locus encoding the skeletal muscle determination genes Mrf4 and Myf5. Genes Dev. 22, 265-276.

Gensch, N., Borchardt, T., Schneider, A., Riethmacher, D. and Braun, T. (2008). Different autonomous myogenic cell populations revealed by ablation of Myf5-expressing cells during mouse embryogenesis. Development 135, 1597-1604.

Giordani, J., Bajard, L., Demignon, J., Daubas, P., Buckingham, M. and Maire, P. (2007). Six proteins regulate the activation of Myf5 expression in embryonic mouse limbs. Proc. Natl. Acad. Sci. U S A. 104, 11310-11315.

Gossen, M. and Bujard, H. (1992). Tight control of gene expression in mammalian cells by tetracycline-responsive promoters. Proc. Natl. Acad. Sci. U S A. 89, 5547-5551.

Grass, S., Arnold, H. H. and Braun, T. (1996). Alterations in somite patterning of Myf-5-deficient mice: a possible role for FGF-4 and FGF-6. Development 122, 141-150.

Haldar, M., Karan, G., Tvrdik, P. and Capecchi, M. R. (2008). Two cell lineages, myf5 and myf5-independent, participate in mouse skeletal myogenesis. Dev. Cell 14, 437-445.

Huang, R., Zhi, Q., Schmidt, C., Wilting, J., Brand-Saberi, B., and Christ, B. (2000). Sclerotomal origin of the ribs. Development 127, 527-532.

Huang, R., Stolte, D., Kurz, H., Ehehalt, F., Cann, G. M., Stockdale, F. E., Patel, K. and Christ, B. (2003). Ventral axial organs regulate expression of myotomal Fgf-8 that influences rib development. Dev. Biol. 255, 30-47.

Kanzler, B., Kuschert, S. J., Liu, Y. H. and Mallo, M. (1998). Hoxa-2 restricts the chondrogenic domain and inhibits bone formation during development of the branchial area. Development 125, 2587-2597.

Kassar-Duchossoy, L., Gayraud-Morel, B., Gomès, D., Rocancourt, D., Buckingham, M., Shinin, V., Tajbakhsh, S. (2004). Mrf4 determines skeletal muscle identity in Myf5:MyoD double-mutant mice. Nature 431, 466-471.

Kaul, A., Köster, M., Neuhaus, H. and Braun, T. (2000). Myf-5 revisited: loss of early myotome formation does not lead to a rib phenotype in homozygous Myf-5 mutant mice. Cell 102, 17-19.

Krumlauf, R. (1994). Hox genes in vertebrate development. Cell 78, 191-201.

Lupien, M., Eeckhoute, J., Meyer, C. A., Wang, Q., Zhang, Y., Li, W., Carroll, J. S., Liu, X. S. and Brown, M. (2008) FoxA1 translates epigenetic signatures into enhancer-driven lineage-specific transcription. Cell 132, 958-970.

Mallo, M. and Brändlin, I. (1997). Segmental identity can change independently in the hindbrain and rhombencephalic neural crest. Dev. Dyn. 210, 146-156.

Mallo, M., Vinagre, T. and Carapuço, M. (2009). The road to the axial formula. Int. J. Dev. Biol. 53, 1469-1481.

Nagashima, H., Sugahara, F., Takechi, M., Ericsson, R., Kawashima-Ohya, Y., Narita, Y. and Kuratani, S. (2009). Evolution of the turtle body plan by the folding and creation of new muscle connections. Science 325, 193-196.

Noyes, M.B., Christensen, R.G., Wakabayashi, A., Stormo, G.D., Brodsky, M.H., Wolfe, S.A. (2008). Analysis of homeodomain specificities allows the family-wide prediction of preferred recognition sites. Cell 133, 1277-1289.

Ohya, Y. K., Usuda, R., Kuraku, S., Nagashima, H. and Kuratani, S. (2006). Unique features of Myf-5 in turtles: nucleotide deletion, alternative splicing, and unusual expression pattern. Evol. Dev. 8, 415-423.

Patapoutian, A., Yoon, J.K., Miner, J.H., Wang, S., Stark, K., Wold, B. (1995). Disruption of the mouse MRF4 gene identifies multiple waves of myogenesis in the myotome. Development 121, 3347-3358.

Pownall, M. E., Gustafsson, M. K. and Emerson, C. P. Jr. (2002). Myogenic regulatory factors and the specification of muscle progenitors in vertebrate embryos. Annu. Rev. Cell. Dev. Biol. 18, 747-783.

Soriano, P. (1997). The PDGF alpha receptor is required for neural crest cell development and for normal patterning of the somites. Development 124, 2691-2700.

Summerbell, D., Halai, C. and Rigby, P. W. (2002). Expression of the myogenic regulatory factor Mrf4 precedes or is contemporaneous with that of Myf5 in the somitic bud. Mech. Dev. 117, 331-335.

Tajbakhsh, S., Rocancourt, D. and Buckingham, M. (1996). Muscle progenitor cells failing to respond to positional cues adopt non-myogenic fates in myf-5 null mice. Nature 384, 266-270.

Tallquist, M. D., Weismann, K. E., Hellström, M., and Soriano, P. (2000). Early myotome specification regulates PDGFA expression and axial skeleton development. Development 127, 5059-5070.

Wellik, D. M. (2007). Hox patterning of the vertebrate axial skeleton. Dev. Dyn. 236, 2454-2463.

Wellik, D. M. and Capecchi, M. R. (2003). Hox10 and Hox11 genes are required to globally pattern the mammalian skeleton. Science 301, 363-367.

Yallowitz, A. R., Gong, K. Q., Swinehart, I. T., Nelson, L. T. and Wellik, D. M. (2009). Non-homeodomain regions of Hox proteins mediate activation versus repression of Six2 via a single enhancer site in vivo. Dev. Biol. 335, 156-165.

Yoon, J. K., Olson, E. N., Arnold, H. H., and Wold, B. J. (1997). Different MRF4 Knockout Alleles Differentially Disrupt Myf-5 Expression: cis-Regulatory Interactions at the MRF4/Myf-5 Locus. Dev. Biol. 188, 349–362.

Zhang, W., Behringer, R. R. and Olson, E. N. (1995). Inactivation of the myogenic bHLH gene MRF4 results in up-regulation of myogenin and rib anomalies. Genes Dev. 9, 1388-1399.

Figure legends

Figure 1. Control rib formation and Myf5/Myf6 expression by Hox genes. **A, B.** *Hoxb6* over-expression in the PSM induces ectopic rib formation. Skeletal staining of wild type (A) and *Dll1-Hoxb6* (B) E18.5 fetuses. Equivalent phenotypes were observed in 4 out of 9 transgenics. **C-J.** Hox groups 6 and 10 modulate regional expression *Myf5* and Myf6. Whole-mount in situ hybridization of wild-type (C, C', E, E'G, G', I, I') *Dll1-Hoxa10* (D, D', H, H') and *Dll1-Hoxb6* (F, F', J, J') mouse embryos with *Myf5* (A–F') and *Myf6* (G-J') probes. Pictures focus on interlimb somites of *Dll1-Hoxa10* embryos and their controls and forelimb somites of *Dll1-Hoxb6* embryos and their controls. Arrows indicate the area of differential expression. Vibratome sections are shown at the arrow level for each marker. Images correspond to embryos at E10.0 (~28-31 somites), except for panels G, H, which are E9.5 (~24 somites). See also Fig. S1.

Figure 2. Hox groups 6 and 10 modulate regional expression of genes in the Myf5/6 pathway. Whole-mount in situ hybridization of wild-type (A-E, G-I, K-M), $Myf5^{\Delta loxp/\Delta loxp}$ (B, B', D, D', F), *Dll1-Hoxa10* (H-J) and *Dll1-Hoxb6* (L-N) mouse embryos with *Myf6* (A-B'), *Pdgfa* (C-D', G-H', K-L') and *Fgf4* (E, F, I, J, M, N) probes. Pictures focus on interlimb somites of *Dll1-Hoxa10* embryos and their controls and forelimb somites of *Dll1-Hoxb6* embryos and their controls. Arrows in A-F indicate the area of conserved expression and in G-N the area of differential expression. Vibratome sections are shown at the arrow level for each marker. Images correspond to embryos at E10.0 (~28-31 somites) except for panels E, F, I, J, M, N, which are E11.0 (~40 somites). See also Fig. S2.

Figure 3. *Myf5*/*Myf6* as functional targets of Hox groups 6 and 10 genes. **A-C**. Rescue of the *Dll1-Hoxa10* phenotype with hypaxial *Myf6*. Skeletal staining of wild type (A), *Dll1-Hoxa10* (B) and *Dll1-Hoxa10::Pax3Pr-Myf6* (C) E18.5 fetuses. A', B' and C' show *Myf6* expression in the corresponding transgenics at E10.0. **D.** Chromatin immunoprecipitation from PSM of E9.5 wild-type mouse embryos using antibodies against Hoxc6 (H6), Hoxa10 (H10) or an unspecific control IgG (IgG), and PCR amplification of the Homology 1 enhancer element (H1) and negative control region (Neg). Inp, input; Blk, blank. These results are representative of three independent experiments. **E.** Luciferase activity from wild type and mutated H1 enhancer (H1enh. and H1*enh., respectively), driven by VP16:Hoxa10, VP16:Hoxb6 or the tetracycline transactivator (tTA), as a control. The activation from the H1 enhancer is statistically significant (VP16:Hoxa10 $p<0.01$ and VP16:Hoxb6 $p<0.04$). The values are presented as the mean and standard error of the triplicates from a representative experiment.

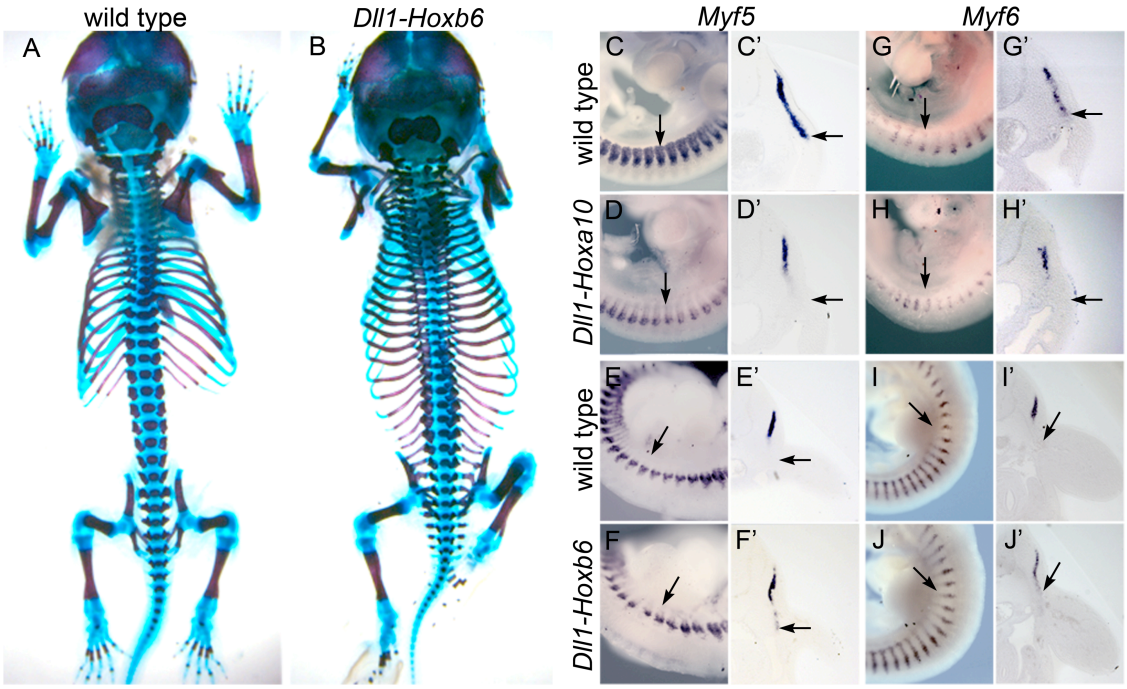
wild type
Dll1-Hoxb6
A
B
Myf5
Myf6
C
C'
G
G'
wild type
D
D'
H
H'
Dll1-Hoxa10
E
E'
I
I'
wild type
F
F'
J
J'
Dll1-Hoxb6

Figure 1

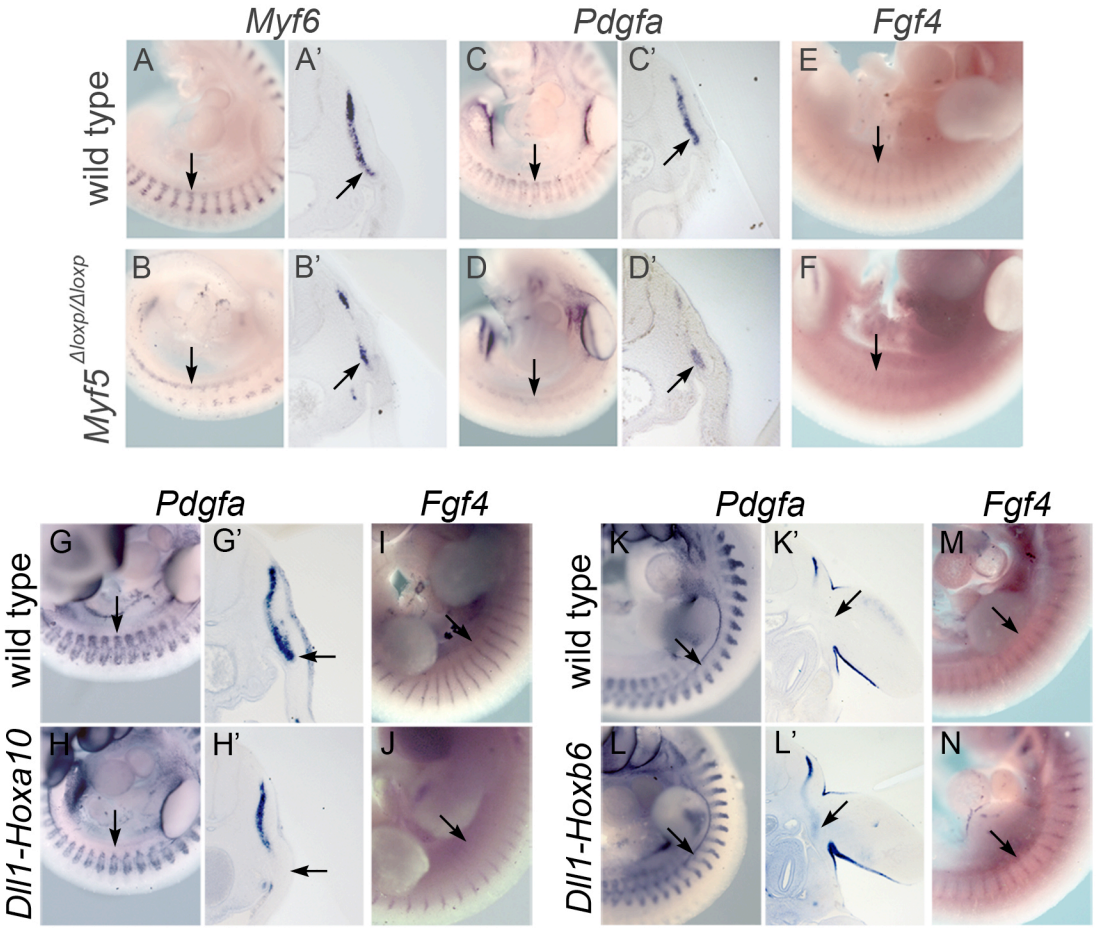
Myf6
Pdgfa
Fgf4
wild type
Myf5 Δloxp/Δloxp
A
A'
B
B'
C
C'
D
D'
E
F
Pdgfa
Fgf4
Pdgfa
Fgf4
wild type
Dll1-Hoxa10
wild type
Dll1-Hoxb6
G
G'
H
H'
I
J
K
K'
L
L'
M
N

Figure 2

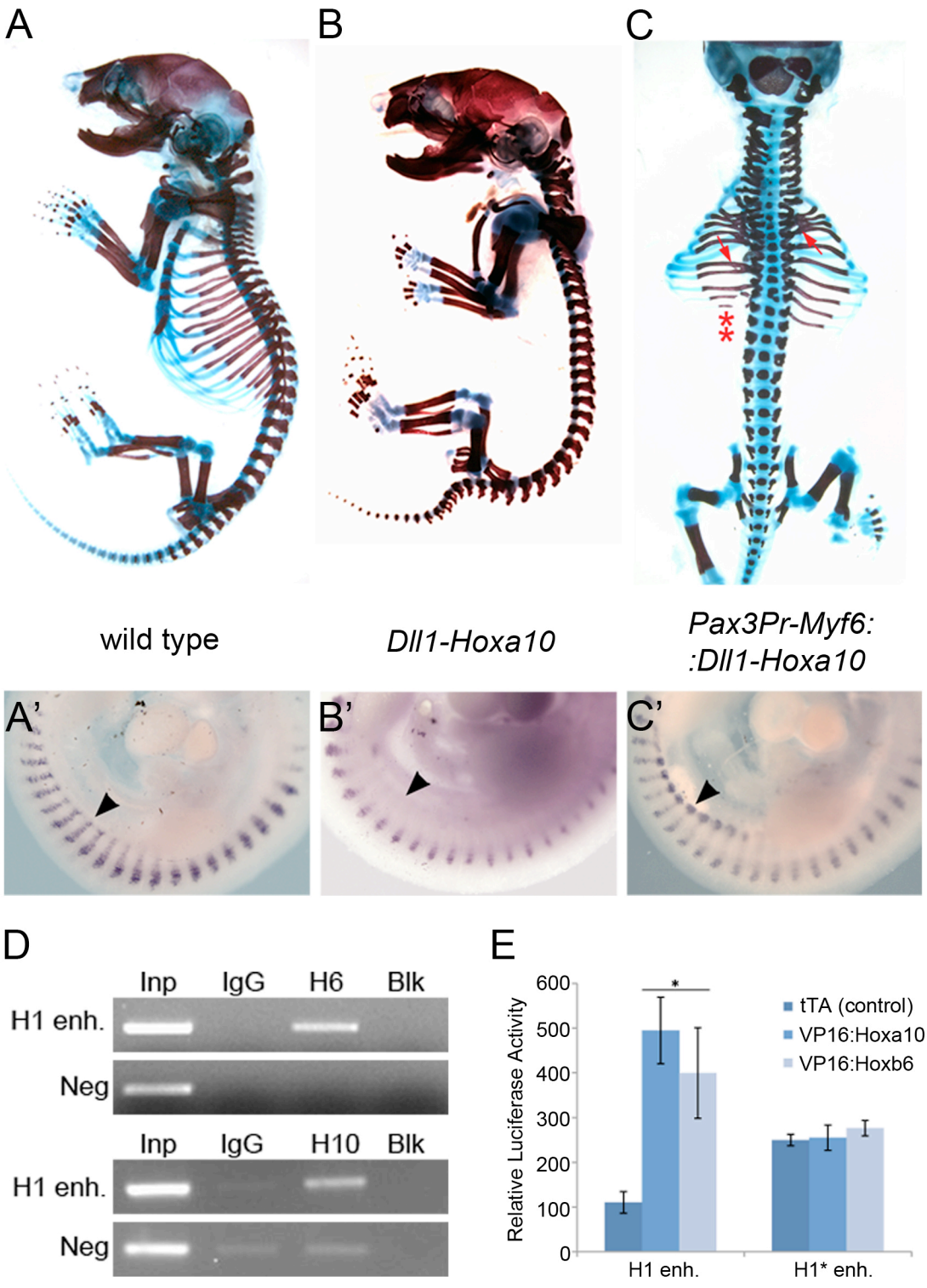
A
B
C
wild type
Dll1-Hoxa10
Pax3Pr-Myf6:
:Dll1-Hoxa10
A'
B'
C'
D
Inp
IgG
H6
Blk
H1 enh.
Neg
Inp
IgG
H10
Blk
H1 enh.
Neg
E
Relative Luciferase Activity
600
500
400
300
200
100
0
*
tTA (control)
VP16:Hoxa10
VP16:Hoxb6
H1 enh.
H1* enh.

Figure 3

Table 1. Comparison of the skeletal phenotype of *Pax3pr-Myf6*, *Dll1-Hoxa10* and *Pax3pr-Myf6::Dll1-Hoxa10* fetuses. Data is represented both as the number embryos showing a particular phenotype/total number embryos analyzed, and as percentages.

	Pax3pr-Myf6	***Dll1-Hoxa10***	***Pax3pr-Myf6: :Dll1-Hoxa10***
Wild type FVB/N phenotype[1]	**7/7 (100%)**	**2/14 (14.29%)**	**4/7 (57.14%)**
Thoracic rib defects	**0/7 (0%)**	**3/14 (21.43%)[2]**	**3/7 (42.86%)[3]**
Complete rib-less phenotype	**0/7 (0%)**	**9/14 (64.29%)**	**0/7 (0%)**

[1] 60% of our FVB/N-derived fetuses contain a small rib in L1.
[2] Variable rib defects in T1, T2 and T13.
[3] See Table S2 for details.

Supplementary Information

Evidence for a myotomal Hox/Myf cascade governing non-autonomous control of rib specification within global vertebral domains

Tânia Vinagre, Natalia Moncaut, Marta Carapuço, Ana Nóvoa, Joana Bom, Moisés Mallo

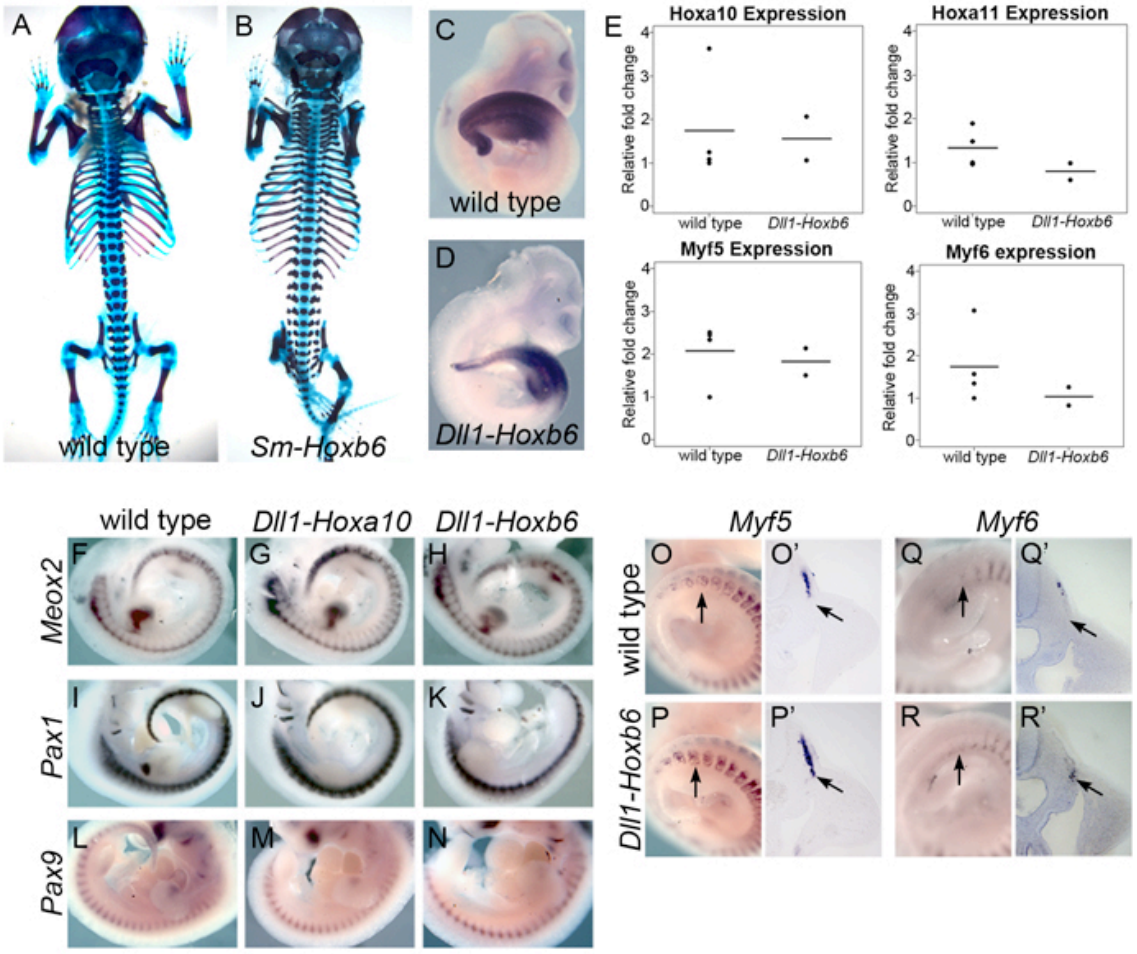

Figure S1. A,B. Mild skeletal phenotype in *Sm-Hoxb6* embryos. Skeletal staining of wild type (A) and *Sm-Hoxb6* (B) E18.5 fetuses. **C-E.** Normal Hox group 10 expression in *Dll-Hoxb6* transgenics. Whole mount *in situ* hybridization of E10.5 wild type (C) and *Dll1-Hoxb6* embryos (D). *Hoxc10* expression is unchanged in *Dll1-Hoxb6* embryos. Quantitative RT-PCR analysis shows normal expression levels of *Hoxa10*, *Hoxa11*, *Myf5* and *Myf6* in PSM and first somites of E10.5 *Dll1-Hoxb6* (n=2) compared with wild type embryos (n=4). GAPDH was used as the endogenous control. Each measurement is the average of duplicate PCR of individual samples. The bar shows the average value for each class. **F-N.** Unchanged expression pattern of several sclerotomal markers in *Dll1-Hoxa10* and *Dll1-Hoxb6* transgenics . Whole mount *in situ* hybridization of E10.5 (F-K) and E11.0 (L-N) wild type (F, I, L), *Dll1-Hoxa10* (G, J, M) and *Dll1-Hoxb6* (H, K, N) embryos: *Meox2* (F-H), *Pax1* (I-K) and *Pax9* (L-N). **O-R.** Hind-limb level expression of *Myf5* and *Myf6*. Whole-mount *in situ* hybridization of E10.0 wild type (O, Q) and *Dll1-*

Hoxb6 embryos (P, R) with *Myf5* (O-P) or *Myf6* (Q, R). The arrows indicate the areas of differential expression. Vibratome sections (O'-R') were done at the arrow level.

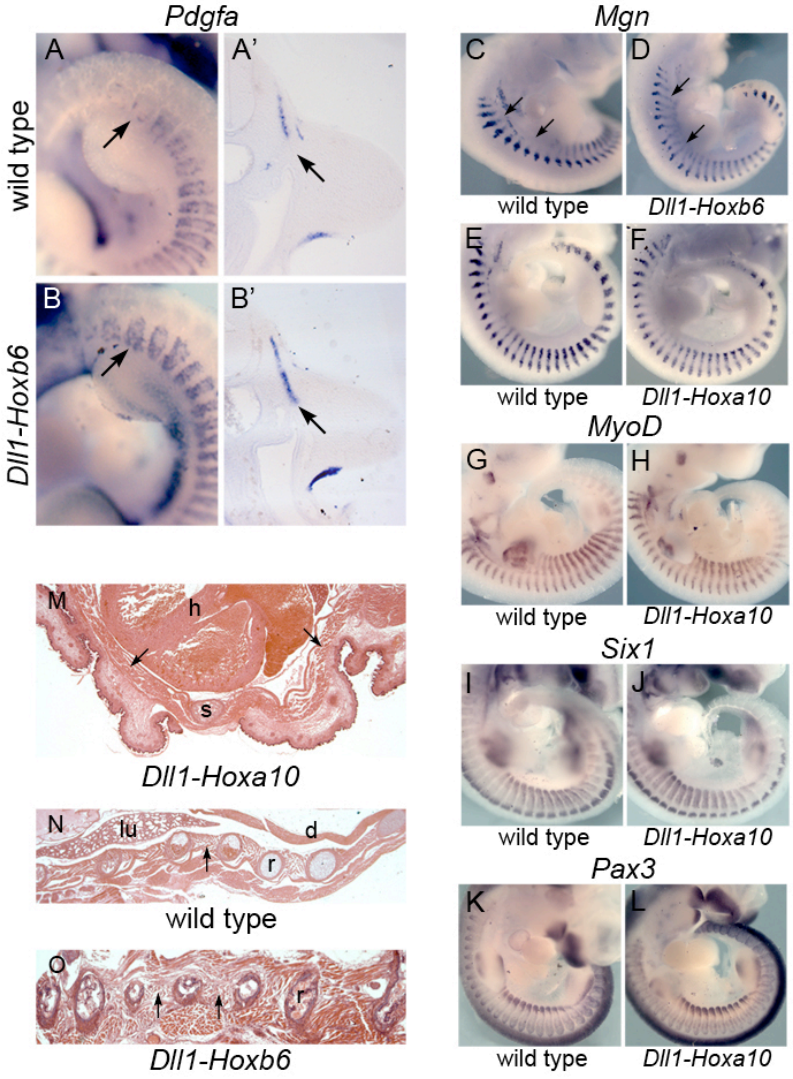

Figure S2. Myotomal and muscle analysis of Hox transgenics. A, B. Hind-limb level expression of *Pdgfa*. Whole-mount *in situ* hybridization of E10.0 wild type (A) and *Dll1-Hoxb6* embryos (B). The arrows indicate the areas of differential expression. Vibratome sections (A', B') were done at the arrow level. **C-L.** Myotomal markers in Hox transgenics. Whole-mount *in situ* hybridization of E10.5 wild type (C, E, G, I, K), *Dll1-Hoxb6* (D) and *Dll1-Hoxa10* (F, H, J, L) embryos with *Mgn* (C-F), *MyoD* (G, H), *Six1* (I, J), *Pax3* (K, L). **M.** Transverse section through the thorax of a E18.5 *Dll1-Hoxa10* (A) embryo, showing muscle tissue (arrows) that reaches the most ventral part of the embryo and attaches to the sternum (s). The picture is oriented with the ventral part of

the specimen at the bottom. **N, O.** Frontal section through the ribcage of a wild type (N) or the neck of a *Dll1-Hoxb6* transgenic (O) embryo at E18.5 showing intercostal muscles (arrows) connecting adjacent ribs (r). Pictures are oriented with rostral to the left and medial to the top. d, diaphragm; h, heart; lu, lung.

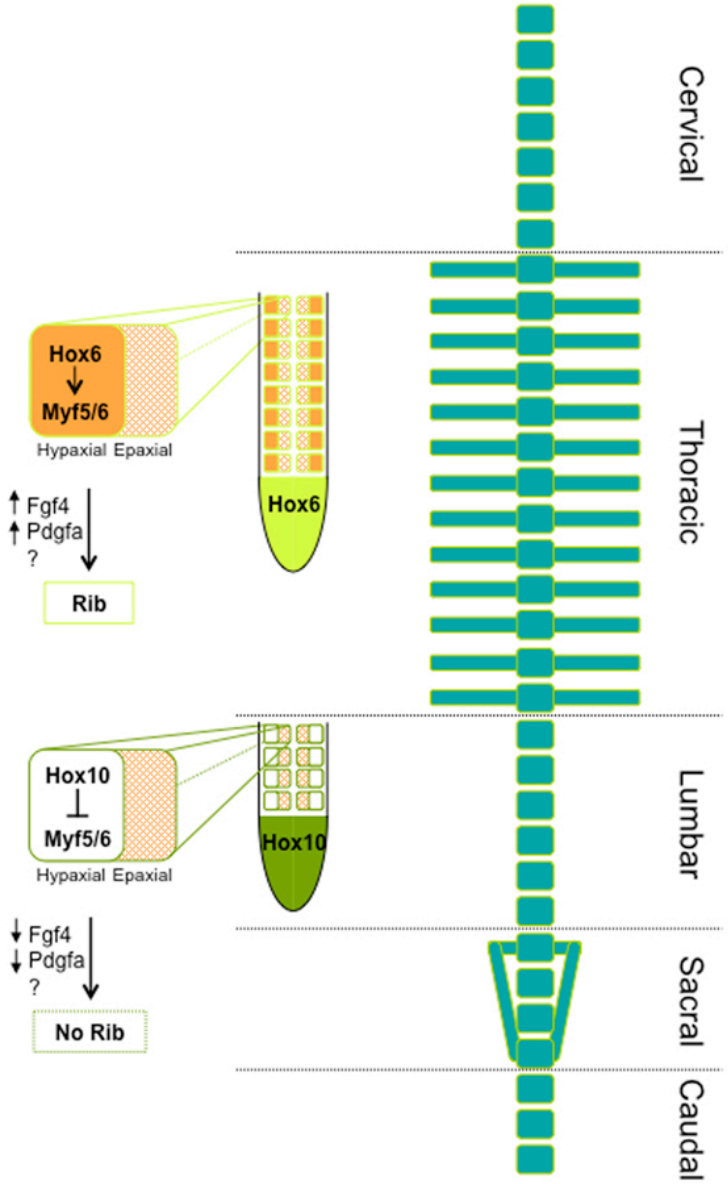

Figure S3. Hox groups 6 and 10 specify global vertebral domains. Schematic representation of Hox-mediated specification of the different vertebral domains of the axial skeleton. On the right panel, the adult cervical, thoracic, lumbar, sacral and caudal vertebral regions of the skeleton are displayed. The left panel shows a representation of the forming somites at different levels. In the prospective thoracic somites, Hox group 6 is activated (light green), thereby up regulating *Myf5* and its downstream effectors *Pdgfa* and *Fgf4* in the hypaxial fraction of the myotome (orange), ultimately leading to rib formation. In the prospective lumbar-caudal somites, Hox group 10 is activated (green),

resulting in the down regulation of *Myf5*, *Pdgfa* and *Fgf4* in the hypaxial myotome (white), leading to inhibition of rib formation in those vertebrae.

Table S1. Skeletal phenotype of *Pax3Pr-Myf6::Dll1-Hoxa10* fetuses. Description of the skeletal abnormalities of the three affected *Pax3Pr-Myf6::Dll1-Hoxa10* out of a total of seven individuals.

	Number of Ribs	**Sternal insertion**	**Proximal rib fusions**	**Proximal Gaps**
#1	12 right side 10 left side	Distorted	Several fusions at different levels	----------
#2	14 right side 12/13 (fused) left side	Distorted	The most caudal ribs are fused together	Proximal gap in T2/T3
#3	12 right side 11 left side	Normal	----------	Proximal gap in T2 /T12